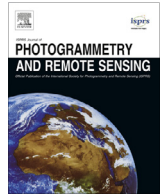




Contents lists available at ScienceDirect

ISPRS Journal of Photogrammetry and Remote Sensing

journal homepage: www.elsevier.com/locate/isprsjprs

Vertical stratification of forest canopy for segmentation of understory trees within small-footprint airborne LiDAR point clouds

Hamid Hamraz^{a,*}, Marco A. Contreras^b, Jun Zhang^a^a Department of Computer Science, University of Kentucky, Lexington, KY 40506, USA^b Department of Forestry, University of Kentucky, Lexington, KY 40506, USA

ARTICLE INFO

Article history:

Received 16 April 2017

Received in revised form 7 June 2017

Accepted 6 July 2017

Keywords:

Remote sensing

Discrete return LiDAR

Multi-story stand

Canopy layering

Individual tree segmentation

ABSTRACT

Airborne LiDAR point cloud representing a forest contains 3D data, from which vertical stand structure even of understory layers can be derived. This paper presents a tree segmentation approach for multi-story stands that stratifies the point cloud to canopy layers and segments individual tree crowns within each layer using a digital surface model based tree segmentation method. The novelty of the approach is the stratification procedure that separates the point cloud to an overstory and multiple understory tree canopy layers by analyzing vertical distributions of LiDAR points within overlapping locales. The procedure does not make a priori assumptions about the shape and size of the tree crowns and can, independent of the tree segmentation method, be utilized to vertically stratify tree crowns of forest canopies. We applied the proposed approach to the University of Kentucky Robinson Forest – a natural deciduous forest with complex and highly variable terrain and vegetation structure. The segmentation results showed that using the stratification procedure strongly improved detecting understory trees (from 46% to 68%) at the cost of introducing a fair number of over-segmented understory trees (increased from 1% to 16%), while barely affecting the overall segmentation quality of overstory trees. Results of vertical stratification of the canopy showed that the point density of understory canopy layers were suboptimal for performing a reasonable tree segmentation, suggesting that acquiring denser LiDAR point clouds would allow more improvements in segmenting understory trees. As shown by inspecting correlations of the results with forest structure, the segmentation approach is applicable to a variety of forest types.

© 2017 International Society for Photogrammetry and Remote Sensing, Inc. (ISPRS). Published by Elsevier B.V. All rights reserved.

1. Introduction

In the past two decades, airborne light detection and ranging (LiDAR) technology has extensively been used for forestry purposes because of its ability to acquire data at unprecedented spatial and temporal resolutions (Ackermann, 1999; Hyyppä et al., 2012; Maltamo et al., 2014; Swatantran et al., 2016). This data is typically captured in the shape of 3D point clouds and can be used to retrieve more detailed tree level information, hence improving the accuracy of forest assessment, monitoring, and management activities (Duncanson et al., 2012; Vastaranta et al., 2011; Weinacker et al., 2004; Wulder et al., 2012). Due to the ability to penetrate vegetation canopy, LiDAR 3D point clouds also contain vertical information from which vegetation structural information can be retrieved (Hall et al., 2011; Lefsky et al., 2002; Maguya et al.,

2014; Reutebuch et al., 2005). This structural information may also include understory layers, which is of great value for various forestry applications and ecological studies (Espírito-Santo et al., 2014; Ishii et al., 2004; Singh et al., 2015; Wing et al., 2012). Although understory trees provide limited financial value and form a minor proportion of total above ground biomass, they influence canopy succession and stand development, create a heterogeneous and dynamic habitat for numerous wildlife species, and are an essential component of forest ecosystems (Antos, 2009; Jules et al., 2008; Moore et al., 2007). However, to obtain individual tree attributes (e.g., location, crown width, height, DBH, volume, biomass) from different canopy layers, accurate and automated tree segmentation approaches that are able to separate tree crowns both vertically and horizontally are required (Duncanson et al., 2014; Ferraz et al., 2012; Shao and Reynolds, 2006; Wang et al., 2008).

Numerous methods for individual tree segmentation within LiDAR data have been developed. Earlier methods use pre-processed data in the form of digital surface models (DSMs) or

* Corresponding author.

E-mail addresses: hhamraz@cs.uky.edu (H. Hamraz), marco.contreras@uky.edu (M.A. Contreras), jzhang@cs.uky.edu (J. Zhang).

canopy height models to segment individual trees (Jing et al., 2012; Koch et al., 2006; Kwak et al., 2007; Popescu and Wynne, 2004; Véga and Durrieu, 2011). These methods have an inherent drawback of missing understory trees by considering only the surface data (Hamraz et al., 2016; Wang et al., 2008). More recent methods process the raw point clouds in order to utilize all horizontal and vertical information and, from the computational viewpoint, can be classified to volumetric or profiler methods. Volumetric methods directly search the 3D volume for the individual trees (Amiri et al., 2016; Ferraz et al., 2012; Lahivaara et al., 2014; Li et al., 2012; Lindberg et al., 2014; Lu et al., 2014; Rahman and Gorte, 2009; Sačkov et al., 2017; Véga et al., 2014). For example, Ferraz et al. (2012) used the mean shift clustering to segment the point cloud and assigned each segment to overstory, understory, or ground vegetation layer. Véga et al. (2014) performed segmentations at different scales and used criteria based on the shape of an ideal tree crown to dynamically select the best set of apices. Sačkov et al. (2017) developed a moving window analysis method to identify potential apices and used several tree allometry rules to increase the likelihood of detecting the actual tree profiles. However, volumetric methods are generally computationally intensive and may be prone to suboptimal solutions due to the large magnitude of the search space.

On the other hand, profiler methods reduce the computational load through a modular process. They typically have a module for vertical segmentation (i.e., to strip the 3D volume to multiple 2D horizontal profiles), a module for horizontal segmentation (i.e., to search the trees within the profiles), and a module to ultimately aggregate the results across the profiles (Ayrey et al., 2017). However, these methods generally lose information about the vertical crown geometry when processing a 2D profile. To minimize information loss due to profiling, other profiler methods have analyzed vertical distribution of LiDAR points to identify 2.5D profiles embodying more information about vertical crown geometry. Wang et al. (2008) searched trees within each profile and used a top-down routine to unify any detected crowns that may be present in different profiles. They analyzed vertical distribution of all LiDAR points globally within a given area to determine the height levels for stripping profiles. However, depending on the vegetation height variability, a globally derived height level may lead to under/over-segmenting tree crowns across the profiles. Other approaches addressed this issue by identifying constrained regions including one or more trees using a preliminary segmentation routine and independently 2.5D profiling each region (Duncanson et al., 2014; Paris et al., 2016; Popescu and Zhao, 2008), yet the final result is dependent on the preliminary segmentation.

Although a number of methods for segmenting individual trees in multi-story stands have been proposed, they are still unable to satisfactorily detect most of the understory trees. Typically, detection rate of dominant and co-dominant (overstory) trees is around or above 90% and detection rate of intermediate and overtopped (understory) trees is below 50%. This inefficacy can be attributed to the reduced amount of LiDAR points penetrating below the main cohort formed by overstory trees (Kükenbrink et al., 2016; Takahashi et al., 2006), although incompleteness of the current approaches to effectively use all vertical and horizontal information also plays a role. In this paper, we present a profiler approach for segmenting crowns of all size trees in multi-story stands. The approach derives height levels locally hence stratifies the point cloud to 2.5D profiles (hereafter referred to as canopy layers). Each canopy layer is sensitive to stand height variability and includes a layer of non-overtopping tree crowns within an unconstrained area. The approach utilizes a DSM-based method as a building block to segment individual tree crowns within each canopy layer.

2. Materials and methods

2.1. Study site and LiDAR campaign

The study site is the University of Kentucky's Robinson Forest (RF, Lat. 37.4611, Long. -83.1555) located in the rugged eastern section of the Cumberland Plateau region of southeastern Kentucky in Breathitt, Perry, and Knott counties (see the [supplementary interactive map](#)). RF features a variable dissected topography (Carpenter and Rumsey, 1976), with moderately steep slopes ranging from 10 to over 100% facing predominately northwest to southeast, with elevations ranging from 252 to 503 m above sea level. Vegetation is composed of a diverse contiguous mixed mesophytic forest made up of approximately 80 tree species with northern red oak (*Quercus rubra*), white oak (*Quercus alba*), yellow-poplar (*Liriodendron tulipifera*), American beech (*Fagus grandifolia*), eastern hemlock (*Tsuga canadensis*) and sugar maple (*Acer saccharum*) as overstory species. Understory species include eastern redbud (*Cercis canadensis*), flowering dogwood (*Cornus florida*), spicebush (*Lindera benzoin*), pawpaw (*Asimina triloba*), umbrella magnolia (*Magnolia tripetala*), and bigleaf magnolia (*Magnolia macrophylla*) (Carpenter and Rumsey, 1976; Overstreet, 1984). Average canopy cover across RF is about 93% with small opening scattered throughout. Most areas exceed 97% canopy cover and recently harvested areas have an average cover as low as 63%. After being extensively logged in the 1920's, RF is considered second growth forest ranging from 80 to 100 years old, and is now protected from commercial logging and mining activities (Department of Forestry, 2007). RF currently covers an aggregate area of ~7440 ha, and includes about 2.5 million ($\pm 13.5\%$) trees, over 60% of which are understory trees (Hamraz et al., 2016, 2017b).

The LiDAR acquisition campaign over RF was performed in the summer of 2013 during leaf-on season (May 28–30) using a Leica ALS60 sensor, which was set at 40° field of view and 200 kHz pulse repetition rate. The sensor was flown at the average altitude of 214 m above ground at the speed of 105 knots with 50% swath overlap. Up to 4 returns were captured per pulse. Using the 95% middle portion of each swath, the resulting LiDAR dataset given the swath overlap has an average density of 50 pt/m². The provider processed the raw LiDAR dataset using the TerraScan software (Terrasolid Ltd, 2012) to classify LiDAR points into ground and non-ground points. Ground points were then used to create a 1-meter resolution digital elevation model (DEM) using the natural neighbor as the fill void method and the average as the interpolation method.

2.2. Tree segmentation approach for multi-layered stands

Using the DEM, normalized heights of the LiDAR points are initially calculated and ground points are removed from further processing. The approach consists of a vertical stratification procedure and a tree segmentation method. The procedure stratifies the top canopy layer of the point cloud by analyzing the vertical distributions of the LiDAR points within overlapping locales and removes the layer from the point cloud. Iterative application of the stratification procedure yields multiple canopy layers. Each canopy layer is independently segmented using a surface-based method. Fig. 1 visualizes the tree segmentation approach.

2.2.1. Vertical stratification

To stratify the top canopy layer, the point cloud is binned into a horizontal grid with a cell width equal to the average footprint (AFP). AFP equals the reciprocal of square root of point density, which itself is defined as the number of points divided by the horizontal area covered by the point cloud (as layers are removed from

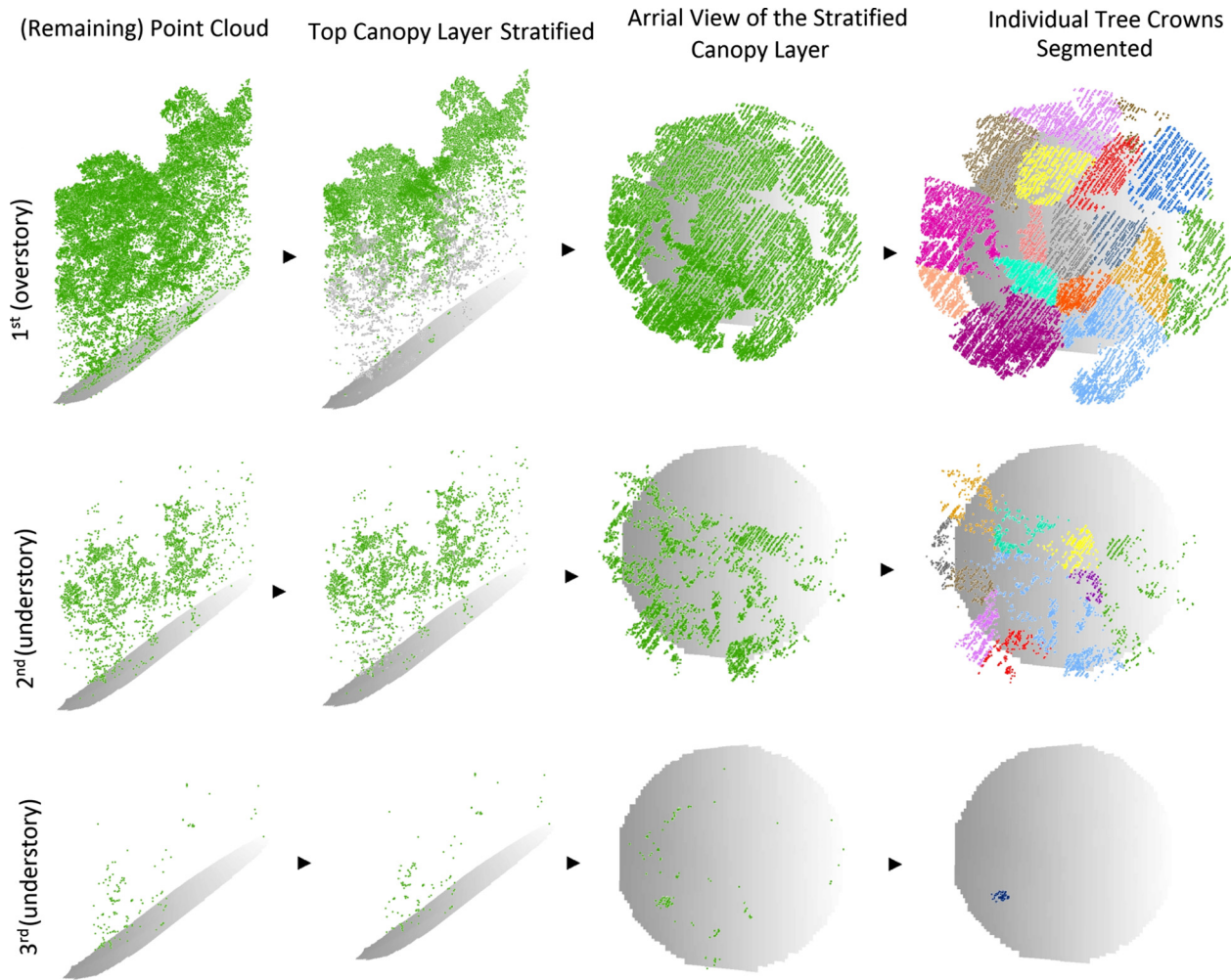


Fig. 1. Illustration of the tree segmentation process in a multi-story stand by stratifying one canopy layer at a time, removing it from the point cloud, and segmenting crowns within each layer. (In the illustration, a number of understory trees seem to be missed within the third canopy layer, which is likely due to the much lower point density compared to the first and second layers).

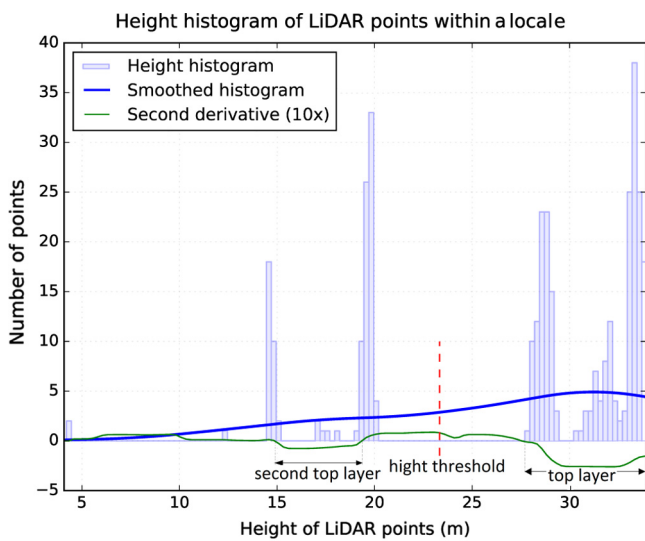


Fig. 2. Height histogram of LiDAR points within a locale including over 100 points used for determining the height threshold for removing the top canopy layer in a cell location.

the point cloud, point density decreases and AFP increases). The height threshold for removing the top layer is determined independently per each grid cell by inspecting the height histogram of all points in a circular locale around the cell. The locale should include sufficient number of points for building an empirical multi-modal distribution but not extending very far to preserve locality. We fixed the radius of the locale to $6 \times \text{AFP}$ (essentially containing about $\pi \times 6^2$ points) and lower bounded it at 1.5 m to prohibit too small locales capturing insufficient spatial structure.

To process a locale, we create a height histogram (bins fixed at 25 cm) of the points in the locale and smooth the histogram to remove variabilities pertaining to vertical structure of a single crown. We used a Gaussian filter with a standard deviation fixed at 5 m for smoothing. Every salient curve in the smoothed histogram, corresponding to a sequence of histogram bins throughout which the second derivative is negative, represents a canopy layer (Popescu and Zhao, 2008; Wang et al., 2008). We choose the midpoint of the gap between the top layer and the second top layer as the height threshold for removing the top canopy layer within the cell location (Fig. 2).

2.2.2. Segmentation of stratified canopy layer

We utilized the DSM-based method introduced by Hamraz et al. (2016) to segment individual trees within a canopy layer. The

segmentation method does not make a priori assumptions about the tree crown shape and size nor spacing between the crowns. It captures this information on-the-fly and adapts the segmentation operation accordingly in order to robustly segment trees in complex stands. The method removes all tree crowns that have an average width of less than 1.5 m or are entirely located below 4 m from the ground (likely ground level vegetation) as noise. The modular design of the approach clearly enables utilizing other segmentation methods as well in case a more customized forest-type specific operation is required.

The height thresholds for removing the top canopy layer are determined using overlapping locales without a priori assumptions about tree crown shape or size. Hence, the canopy layer smoothly adjusts to incorporate vertical variabilities of crowns within an unconstrained area to minimize under/over-segmenting tree crowns (Fig. 1), which is the major novelty of the proposed approach. Because the segmentation method also does not make a priori assumptions about the stand structure, the combination is a robust tree segmentation approach for a multi-layered stand that can be applied to different forest types.

2.3. Approach evaluation

2.3.1. Field data

Throughout the entire RF, 270 regularly distributed (grid-wise every 384 m) circular plots of 0.04 ha in size, centers of which were georeferenced with 5 m accuracy, were field surveyed during the summer of 2013 (see the [supplementary interactive map](#)). Within each plot, DBH (cm), tree height (m), species, crown class (dominant, co-dominant, intermediate, overtopped), tree status (live, dead), and stem class (single, multiple) were recorded for all trees with DBH > 12.5 cm. In addition, horizontal distance and azimuth from plot center to the face of each tree at breast height were collected to create a stem map. Site variables including slope, aspect, and slope position were also recorded for each plot. Average height of overstory trees was 25.5 m with a standard deviation of 5.3 m and average height of understory trees was 17.2 m with a standard deviation of 4.3 m. Table 1 shows a plot level summary.

2.3.2. Evaluation method

LiDAR point clouds over each of the 270 field-surveyed plots included a 4.7-m buffer for capturing complete crowns of border trees using the proposed tree segmentation approach. The evaluation method assigns a score to each pair of LiDAR-derived tree location, assumed to be the apex of the segmented crown, and stem

location measured in the field according to the tree height difference (should be less than 30%) and the leaning angle (should be less than 15° from nadir) between the crown apex and the stem location. The method selects the set of pairs with the maximum total score where each crown or stem location appears not more than once using the Hungarian assignment algorithm and regards the set as the matched trees (Hamraz et al., 2016; Kuhn, 1955). The number of matched trees (MT) is an indication of the tree segmentation quality. The number of unmatched stem map locations (omission errors – OE) and unmatched LiDAR-derived crown apexes that are not in the buffer area (commission errors – CE) indicate under- and over-segmentation, respectively. The accuracy of the approach is calculated in terms of recall (Re – measure of tree detection rate), precision (Pr – measure of correctness of detected trees), and F-score (F – combined measure) using the following equations (Manning et al., 2008):

$$Re = \frac{MT}{MT + OE} \quad (1)$$

$$Pr = \frac{MT}{MT + CE} \quad (2)$$

$$F = 2 \times \frac{Re \times Pr}{Re + Pr} \quad (3)$$

We evaluated the accuracy of the approach with and without canopy stratification (equivalent to the bare DSM-based method used in the approach) to assess the utility of the canopy stratification procedure. We conducted two-tailed paired T-tests to compare the DSM-based and the stratification-enabled approach over nine accuracy metrics, i.e., precision, recall, and F-score for overstory, understory, and all trees. Our sample of 270 plots is large enough to satisfy the assumptions of the T-test even if the data is not normally distributed. We also inspected the Pearson correlations of the accuracy metrics for the stratification-enabled approach with different plot level parameters. These correlation relations help investigate how the performance of the approach is affected according to the terrain and stand variability across RF.

3. Results

3.1. Vertical stratification

The stratification procedure identified three (68.2%) or four (24.1%) canopy layers for most of the 270 plots with an expected

Table 1
Summary of plot level data collected from the 270 plots in Robinson Forest.

Plot-Level Metric		Min	Max	Avg.	Total	Percent of total
Slope	(%)	0	93	50		
Aspect	°	2	360	179		
Tree count		2	41	14.7	3971	
Dominant		0	3	0.5	130	3.3
Co-dominant		0	10	3.5	954	24.0
Intermediate		0	34	5.5	1481	37.3
Overtopped		0	19	4.3	1152	29.0
Dead		0	7	0.9	254	6.4
Mean tree height	(m)	13.9	28.8	19.5		
Dominant	(m)	15.6	40.8	27.8		
Co-dominant	(m)	10.6	37.8	25.0		
Intermediate	(m)	11.2	32.0	19.9		
Overtopped	(m)	7.1	24.8	15.8		
Dead	(m)	0.0	26.3	9.5		
Standard deviation of tree heights	(m)	1.2	12.4	5.5		
Species count		1	12	6.0	43	
Shannon diversity index		0.0	2.25	1.50		

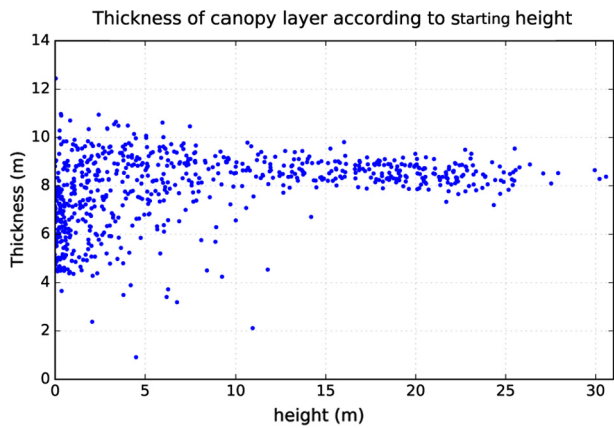


Fig. 3. Thickness of canopy layer according to starting height of the layer.

number of canopy layers of 3.16. Any layer located below 4 m for its entirety was excluded because it likely represents ground level vegetation, though any of the remaining layers may extend below 4 m and even touch the ground. Starting height and thickness of a canopy layer are defined as the median over all grid cells used to stratify the layer (Fig. 2). The average starting height of a canopy layer ranged from 0.3 to 18.2 m and the average thickness of a layer ranged between 6.1 and 8.8 m. Also, the average point density of a layer ranged between 0.44 and 42.08 pt/m². The average starting height, thickness, and point density of the entire canopy (all layers aggregated) were 1.4 m, 24.8 m, and 47.45 pt/m², respectively. The average point density of the entire canopy agrees with the average point density of the initial LiDAR dataset of 50 pt/m² given that ground and ground level vegetation returns were removed.

Thickness of a canopy layer seemed to be unrelated to its starting height except only for very low starting heights (Fig. 3), which is likely associated with layers formed by very small trees. Dependence of a canopy layer thickness on the number of layers preceding it and its independence to height is likely due to the fact that tree crowns within a canopy layer adapt their shape to maximize light exposure (Duursma and Mäkelä, 2007; OSADA and TAKEDA, 2003), and light exposure is related to the amount of light already intercepted by preceding canopy layers rather than the height of the layer.

3.2. Tree segmentation accuracy

On average for the 270 sample plots, results from the DSM-based tree segmentation show higher precisions by 5–15% while the stratification-enabled approach shows higher recalls by 5–22% and higher F-scores by up to 12% (Fig. 4). When comparing the stratification-enabled against the DSM-based approach using T-tests (Table 3), all metrics except F-score for overstory trees showed significant ($P < 0.0001$) changes. Recall and precision for understory trees showed the largest changes: an increase from 46% to 68% (MSE = 10.04) and a decrease from 99% to 84% (MSE = 3.97), respectively. Overall, the stratification-enabled tree segmentation approach shows improvements in F-scores for understory (from 61% to 73%, MSE = 1.70) as well as all trees (from 70% to 77%, MSE = 0.66), while barely affecting F-score for overstory trees compared with the DSM-based approach (Fig. 4).

We inspected the correlations of terrain slope and aspect, stem density, Shannon diversity index of tree species, average and standard deviation of tree heights, average height difference of overstory and understory trees, and ratio of the number of overstory to understory trees in a plot with recalls and precisions of the

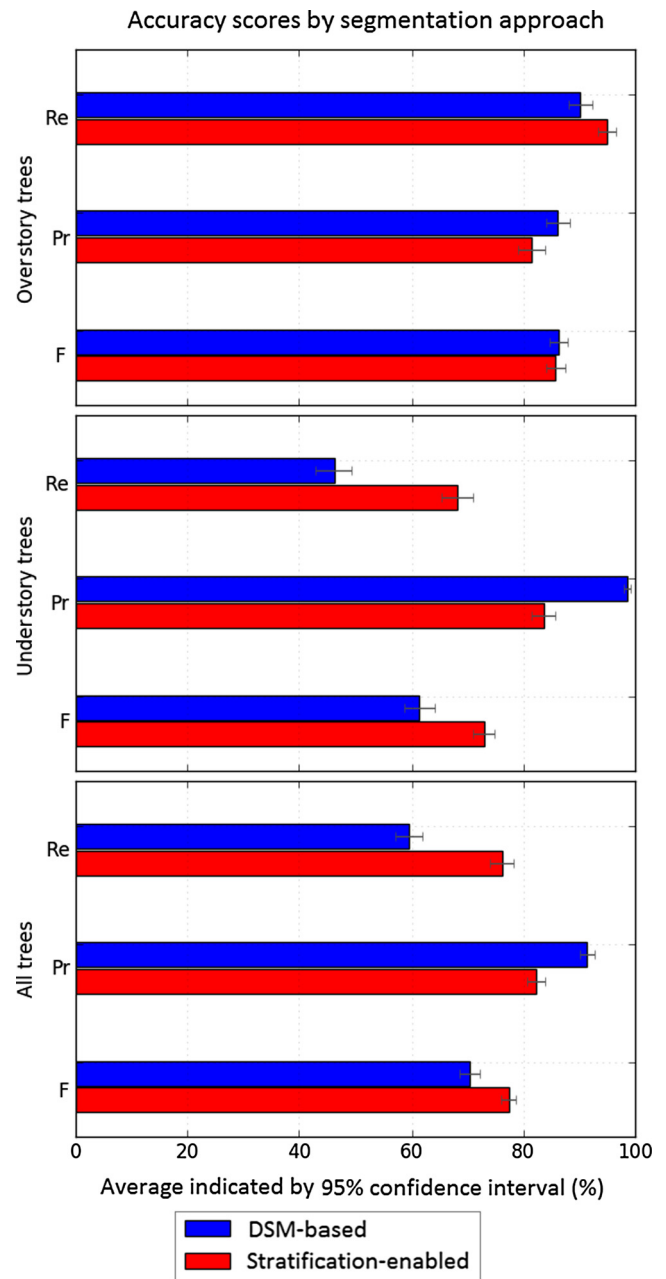


Fig. 4. Average segmentation accuracies over 270 sample plots grouped by crown class.

stratification-enabled approach. We observed a significant but weak negative correlation between plot slope and recall of understory trees ($P = 0.006$, $r = -0.17$). This correlation indicates that detection of understory trees in sloped terrain is slightly more difficult. Furthermore, significant weak correlations were observed between stem density and recall ($P = 0.0006$, $r = -0.21$), precision ($P = 0.009$, $r = +0.16$) of understory trees as well as precision ($P = 0.009$, $r = +0.16$) of overstory trees. Average tree height in a plot showed significant weak correlations with recall ($P < 0.0001$, $r = +0.25$) and precision ($P = 0.007$, $r = -0.17$) of understory trees as well as recall ($P = 0.0001$, $r = +0.23$) of overstory trees. These observations indicate trees in denser stands and/or smaller trees are harder to detect while the detected trees are slightly less prone to over-segmentation. Standard deviation of tree heights also had significant weak negative correlations with precision of understory ($P = 0.0007$, $r = -0.21$) and overstory ($P = 0.009$, $r = -0.16$) trees.

This observation indicates that large variability in tree heights slightly degrades segmentation quality, which is likely associated with the performance of the stratification procedure. Average height difference of overstory and understory trees also had significant weak negative correlations with recall of understory trees ($P = 0.002$, $r = -0.19$) and precision of overstory trees ($P = 0.004$, $r = -0.18$). This reaffirms the fact that smaller (understory) trees are harder to detect and larger (overstory) trees are more prone to over-segmentation while it also indicates the robustness of the stratification procedure because the tighter gap between overstory and understory seemed not to degrade performance metrics. Lastly, the ratio of overstory to understory trees showed a relatively stronger negative correlation with precision of understory trees ($P < 0.0001$, $r = -0.35$). A larger number of overstory trees means more occlusion for understory trees resulting in lower point density and potentially less homogeneity in point distribution of understory canopy layers, making understory trees more prone to over-segmentation. This observation is mainly associated with the low point density of understory canopy layers rather than the segmentation approach.

4. Discussions

Although the stratification procedure is in theory robust and applicable to a variety of stand structures, it increased the number of over-segmentations by a fair amount (5–15%) depending on the crown class in our study. Inspecting Fig. 2, vertical over-segmentation is likely when the smoothing operation cannot remove the vertical variability pertaining to a single crown. We tried to alleviate this problem by adaptively adjusting the size of the smoothing window according to vegetation height so as to reach a more favorable trade-off between under- and over-segmentations, yet our attempt did not make improvements. We also tried a post-processing module to merge the likely over-segmentations back to the crown they belong to, but this attempt also resulted in no improvements. We speculate adjusting the window size based on the field observations of a forested area in question is the best path to follow to tackle this problem.

Overall, the stratification procedure improved tree segmentation accuracy as benchmarked against a recently developed

DSM-based segmentation method (Fig. 4, Hamraz et al., 2016). However, this overall improvement is majorly composed of a strong increase in detection rate and a moderate decrease in correctness of the detected understory trees. Detecting more trees likely increased the chance of over-segmentation of the detected trees, and this was strongly pronounced for understory trees compared with overstory trees. This observation indicates an increased sensitivity of the stratification-enabled approach to segment understory trees while barely affecting the segmentation of overstory trees compared with the DSM-based method, which is also an indication of the sound operation of the stratification procedure. Correlations of the accuracy metrics with plot level metrics over a forest with a complex and highly variable structure were insignificant and/or weak. This observation evidences that the stratification-enabled approach can also be used for multi-layered tree segmentation of different forest types.

To understand the vertical structure of tree canopy layers of forested landscapes (Leiterer et al., 2015; Whitehurst et al., 2013), the proposed stratification procedure can be applied independent of the tree segmentation method. As observed, average thickness and point density decreases with lower canopy layers (Table 2). Specifically, the third and fourth canopy layers, where a large number of understory trees are found, have an average density lower than 1 pt/m^2 (Table 2). Such low density is below the optimal point density ($\sim 4 \text{ pt/m}^2$) for segmenting individual trees (Evans et al., 2009; Jakubowski et al., 2013; Wallace et al., 2014), which is the main reason for inferior tree segmentation accuracy of understory trees compared with overstory trees. Moreover, lower canopy layers are more tightly placed compared with higher canopy layers as also shown by Whitehurst et al. (2013), which might have made stratification of the layers more challenging and increased the chances of under/over-segmentation of small understory trees.

As reported by Kükenbrink et al. (2016), at least 25% of canopy volume remain uncovered even in small-footprint airborne LiDAR acquisition campaigns, which concurs with suboptimal point density of lower canopy layers for tree segmentation in our study. If, however, our initial point cloud was a few times denser, the two lower canopy layers might have neared the optimal density, likely boosting segmentation accuracy of understory trees. In a

Table 2
Summary statistics of the canopy layers stratified within the 270 sample plots.

Canopy Layer	Plots ^a	Starting Height (m)		Thickness (m)		Point Density (pt/m ²)	
		Avg.	S.D.	Avg.	S.D.	Avg.	S.D.
1	0.00%	18.16	4.53	8.18	0.38	42.08	17.42
2	7.78%	4.23	2.58	8.76	0.99	5.02	3.23
3	68.15%	0.47	1.03	6.44	1.35	0.84	0.79
4	24.07%	0.34	1.39	6.14	1.82	0.44	0.80
Aggregate	100.00%	1.38	1.41	24.85	4.26	47.45	20.13

^a Plots having as many number of canopy layers.

Table 3
Summary of two-tailed paired T-tests assessing the improvement of canopy stratification for tree segmentation.

Tree Class	Accuracy Metric	Samples Used	MSE	T-Score	P-Value	Average Improvement
Overstory	Re	269	0.438	45.67	<0.0001	+4.68%
	Pr	269	0.726	32.95	<0.0001	-4.58%
	F	268	0.005	0.40	0.53	-0.64%
Understory	Re	267	10.035	454.17	<0.0001	+22.10%
	Pr	265	3.969	233.19	<0.0001	-15.05%
	F	261	1.698	90.73	<0.0001	+11.52%
All	Re	270	5.440	473.70	<0.0001	+16.56%
	Pr	270	1.744	175.00	<0.0001	-8.98%
	F	269	0.655	76.39	<0.0001	+6.98%

concurrent study, we modeled how point density of lower canopy layers decreases and estimated that a point cloud density of about 170 pt/m² is required to segment understory trees within as deep as the third canopy layer with accuracies similar to overstory trees (Hamraz et al., 2017a). Such dense LiDAR campaigns are slowly becoming more affordable given the advancements of the sensor technology and platforms as exemplified by recent emergence of single photon LiDAR technology providing 10x efficiency boost (Swatantran et al., 2016; Wallace, 2017).

Lastly, a few similar studies processed raw LiDAR point clouds and reported accuracy metrics for segmentation of understory trees. In a Norway spruce dominated forest, Solberg et al. (2006) detected 66% of the trees (dominant 93%, co-dominant 63%, intermediate 38%, and overtopped 19%) with a commission error of 26%. Paris et al. (2016) detected more than 90% of overstory and about 77% of understory trees with a commission rate of 7% in conifer sites located in the Southern Italian Alps. However, due to tree crown architecture, segmenting trees in conifer stands is relatively simpler and studies have showed better performance compared to deciduous or mixed stands (Hu et al., 2014; Vauhkonen et al., 2011). In a deciduous stand at Smithsonian Environmental Research Center, Maryland, Duncanson et al. (2014) detected 70% of dominant (0% commissions), 58% of co-dominant (45% commissions), 35% of intermediate (166% commissions), and 21% of overtopped (29% commissions) trees. Ferraz et al. (2012) detected 99.3% of dominant, 92.6% of co-dominant, 65.7% of intermediate, and 14.5% of overtopped Eucalyptus trees in a Portuguese forest with an overall commission rate of 9.2%. In another deciduous stand in Eastern France, Véga et al. (2014) detected 100% and 44% of overstory and understory trees with 27% and 3% commissions, respectively. The detection rate of our stratification-enabled tree segmentation approach was 95% for overstory trees and 68% for understory trees with commission rates of ~17% in a deciduous forest. These results show improvements, especially in segmenting understory trees, bearing the caveat that aforementioned studies were conducted in different sites using different LiDAR acquisition parameters with slightly different field surveying protocols and evaluation methods.

5. Conclusions

Small-footprint LiDAR data covering forested areas contain a wealth of information of both horizontal and vertical vegetation structure that can be utilized to enhance various forestry applications and ecological studies. In this paper, we presented a profiler approach that stratified the raw point cloud extended over an unconstrained area to its tree canopy layers without making a priori assumptions about tree shape and size, and utilized a DSM-based tree crown segmentation method as a building block for each layer to segment all sized trees in a multi-story deciduous stand. The proposed canopy stratification procedure can also be applied independent of the crown segmentation method in order to vertically stratify canopy to flexible layers of tree crowns over unconstrained areas. Statistical analyses showed overall improvements in segmentation accuracy of understory trees without any noticeable change in the accuracy of overstory trees, which was the main objective of using canopy stratification as a module for tree segmentation. As evidenced by inspecting correlations of accuracy with plot level metrics, the approach can be applied to segment trees within different forest types.

The modular process of our segmentation approach allowed us to study individual canopy layers. We observed that the point densities of the lower canopy layers were suboptimal for segmentation of individual understory trees. It is expected that acquiring denser LiDAR point clouds brings the point density of lower canopy layers

closer to optimal value, likely resulting in additional improvements in the segmentation of understory trees. The result presented indicates this work is a promising step forward toward correctly retrieving and modeling all individual (overstory and understory) trees of a natural forest using small-footprint LiDAR data.

Data availability

The datasets generated during and/or analyzed during the current study are available from the corresponding author on reasonable request.

Acknowledgments

This work was supported by: (1) the Department of Forestry at the University of Kentucky and the McIntire-Stennis project KY009026 Accession 1001477, (ii) the Kentucky Science and Engineering Foundation under the grant KSEF-3405-RDE-018, and (iii) the University of Kentucky Center for Computational Sciences. The authors would also like to thank Chase Clark for preparing the 3D visualization in Fig. 1 and the supplementary KML file of RF and the plots.

Appendix A. Supplementary material

Supplementary data associated with this article can be found, in the online version, at <http://dx.doi.org/10.1016/j.isprsjprs.2017.07.001>. These data include Google maps of the most important areas described in this article.

References

- Ackermann, F., 1999. Airborne laser scanning—present status and future expectations. *ISPRS J. Photogramm. Remote Sens.* 54, 64–67.
- Amiri, N., Yao, W., Heurich, M., Krzystek, P., Skidmore, A.K., 2016. Estimation of regeneration coverage in a temperate forest by 3D segmentation using airborne laser scanning data. *Int. J. Appl. Earth Obs. Geoinf.* 52, 252–262.
- Antos, J., 2009. Understory plants in temperate forests. In: *Forests and Forest Plants*. Eolss Publishers Co Ltd, Oxford, pp. 262–279.
- Ayrey, E., Fraver, S., Kershaw Jr., J.A., Kenefic, L.S., Hayes, D., Weiskittel, A.R., Roth, B. E., 2017. Layer stacking: a novel algorithm for individual forest tree segmentation from LiDAR point clouds. *Can. J. Remote. Sens.*, 1–13
- Carpenter, S.B., Rumsey, R.L., 1976. *Trees and shrubs of Robinson Forest Breathitt County, Kentucky*. Castanea, 277–282.
- Department of Forestry, 2007. *Robinson Forest: a facility for research, teaching, and extension education*. In: University of Kentucky.
- Duncanson, L., Cook, B., Hurtt, G., Dubayah, R., 2014. An efficient, multi-layered crown delineation algorithm for mapping individual tree structure across multiple ecosystems. *Remote Sens. Environ.* 154, 378–386.
- Duncanson, L., Dubayah, R., Hurtt, G., Pinto, N., Cook, B., Swatantran, A., 2012. How important is individual tree information for biomass modeling and mapping? In: *AGU Fall Meeting Abstracts*, p. 0353.
- Duursma, R., Mäkelä, A., 2007. Summary models for light interception and light-use efficiency of non-homogeneous canopies. *Tree Physiol.* 27, 859–870.
- Espírito-Santo, F.D., Gloor, M., Keller, M., Malhi, Y., Saatchi, S., Nelson, B., Junior, R.C. O., Pereira, C., Lloyd, J., Frolking, S., 2014. Size and frequency of natural forest disturbances and the Amazon forest carbon balance. *Nat. Commun.* 5.
- Evans, J.S., Hudak, A.T., Faux, R., Smith, A., 2009. Discrete return lidar in natural resources: Recommendations for project planning, data processing, and deliverables. *Remote Sens.* 1, 776–794.
- Ferraz, A., Bretar, F., Jacquemoud, S., Gonçalves, G., Pereira, L., Tomé, M., Soares, P., 2012. 3-D mapping of a multi-layered Mediterranean forest using ALS data. *Remote Sens. Environ.* 121, 210–223.
- Hall, F.G., Bergen, K., Blair, J.B., Dubayah, R., Houghton, R., Hurtt, G., Kellndorfer, J., Lefsky, M., Ranson, J., Saatchi, S., 2011. Characterizing 3D vegetation structure from space: Mission requirements. *Remote Sens. Environ.* 115, 2753–2775.
- Hamraz, H., Contreras, M.A., Zhang, J., 2016. A robust approach for tree segmentation in deciduous forests using small-footprint airborne LiDAR data. *Int. J. Appl. Earth Obs. Geoinf.* 52, 532–541.
- Hamraz, H., Contreras, M.A., Zhang, J., 2017a. Forest understory trees can be segmented accurately using sufficiently dense airborne laser scanning point clouds. *Nature Scientific Reports*. arXiv preprint arXiv:1702.06188.
- Hamraz, H., Contreras, M.A., Zhang, J., 2017b. A scalable approach for tree segmentation within small-footprint airborne LiDAR data. *Comput. Geosci.* 102, 139–147.

- Hu, B., Li, J., Jing, L., Judah, A., 2014. Improving the efficiency and accuracy of individual tree crown delineation from high-density LiDAR data. *Int. J. Appl. Earth Obs. Geoinf.* 26, 145–155.
- Hyyppä, J., Holopainen, M., Olsson, H., 2012. Laser scanning in forests. *Remote Sens.* 4, 2919–2922.
- Ishii, H.T., Tanabe, S.-I., Hiura, T., 2004. Exploring the relationships among canopy structure, stand productivity, and biodiversity of temperate forest ecosystems. *For. Sci.* 50, 342–355.
- Jakubowski, M.K., Guo, Q., Kelly, M., 2013. Tradeoffs between lidar pulse density and forest measurement accuracy. *Remote Sens. Environ.* 130, 245–253.
- Jing, L., Hu, B., Li, J., Noland, T., 2012. Automated delineation of individual tree crowns from LiDAR data by multi-scale analysis and segmentation. *Photogramm. Eng. Remote Sens.* 78, 1275–1284.
- Jules, M.J., Sawyer, J.O., Jules, E.S., 2008. Assessing the relationships between stand development and understory vegetation using a 420-year chronosequence. *For. Ecol. Manage.* 255, 2384–2393.
- Koch, B., Heyder, U., Weinacker, H., 2006. Detection of individual tree crowns in airborne LiDAR data. *Photogramm. Eng. Remote Sens.* 72, 357–363.
- Kuhn, H.W., 1955. The Hungarian method for the assignment problem. *Naval Res. Logist. Quart.* 2, 83–97.
- Kükenbrink, D., Schneider, F.D., Leiterer, R., Schaepman, M.E., Morsdorf, F., 2016. Quantification of hidden canopy volume of airborne laser scanning data using a voxel traversal algorithm. *Remote Sens. Environ.*
- Kwak, D.-A., Lee, W.-K., Lee, J.-H., Biging, G.S., Gong, P., 2007. Detection of individual trees and estimation of tree height using LiDAR data. *J. For. Res.* 12, 425–434.
- Lahivaara, T., Seppänen, A., Kaipio, J.P., Vauhkonen, J., Korhonen, L., Tokola, T., Maltamo, M., 2014. Bayesian approach to tree detection based on airborne laser scanning data. *IEEE Trans. Geosci. Remote Sens.* 52, 2690–2699.
- Lefsky, M.A., Cohen, W.B., Parker, G.G., Harding, D.J., 2002. LiDAR remote sensing for ecosystem studies. *BioScience* 52, 19–30.
- Leiterer, R., Furrer, R., Schaepman, M.E., Morsdorf, F., 2015. Forest canopy-structure characterization: A data-driven approach. *For. Ecol. Manage.* 358, 48–61.
- Li, W., Guo, Q., Jakubowski, M.K., Kelly, M., 2012. A new method for segmenting individual trees from the LiDAR point cloud. *Photogramm. Eng. Remote Sens.* 78, 75–84.
- Lindberg, E., Eysn, L., Hollaus, M., Holmgren, J., Pfeifer, N., 2014. Delineation of tree crowns and tree species classification from full-waveform airborne laser scanning data using 3-D ellipsoidal clustering. *IEEE J. Sel. Top. Appl. Earth Observ. Remote Sens.* 7, 3174–3181.
- Lu, X., Guo, Q., Li, W., Flanagan, J., 2014. A bottom-up approach to segment individual deciduous trees using leaf-off lidar point cloud data. *ISPRS J. Photogramm. Remote Sens.* 94, 1–12.
- Maguya, A.S., Junttila, V., Kauranne, T., 2014. Algorithm for extracting digital terrain models under forest canopy from airborne LiDAR data. *Remote Sens.* 6, 6524–6548.
- Maltamo, M., Næsset, E., Vauhkonen, J., 2014. Forestry Applications of airborne laser scanning: concepts and case studies. *Manage. For. Ecosys.*
- Manning, C.D., Raghavan, P., Schütze, H., 2008. *Introduction to Information Retrieval*. Cambridge University Press, Cambridge.
- Moore, P., Van Miegroet, H., Nicholas, N., 2007. Relative role of understory and overstory in carbon and nitrogen cycling in a southern Appalachian spruce-fir forest AES Publication 7863. Utah Agricultural Experiment Station, Utah State University, Logan, Utah. *Can. J. For. Res.* 37, 2689–2700.
- Osada, N., Takeda, H., 2003. Branch architecture, light interception and crown development in saplings of a plagiotropically branching tropical tree, *Polyalthia jenkinsii* (Annonaceae). *Ann. Bot.* 91, 55–63.
- Overstreet, J., 1984. *Robinson Forest Inventory*. University of Kentucky, Lexington, Kentucky, Department of Forestry.
- Paris, C., Valduga, D., Bruzzone, L., 2016. A hierarchical approach to three-dimensional segmentation of LiDAR data at single-tree level in a multilayered forest. *IEEE Trans. Geosci. Remote Sens.* 54, 4190–4203.
- Popescu, S.C., Wynne, R.H., 2004. Seeing the trees in the forest. *Photogramm. Eng. Remote Sens.* 70, 589–604.
- Popescu, S.C., Zhao, K., 2008. A voxel-based lidar method for estimating crown base height for deciduous and pine trees. *Remote Sens. Environ.* 112, 767–781.
- Rahman, M., Gorte, B., 2009. Tree crown delineation from high resolution airborne lidar based on densities of high points. In: *Proceedings ISPRS Workshop Laserscanning 2009*, September 1–2, France, IAPRS, XXXVIII (3/W8), 2009: ISPRS.
- Reutebuch, S.E., Andersen, H.-E., McGaughey, R.J., 2005. Light detection and ranging (LiDAR): an emerging tool for multiple resource inventory. *J. Forest.* 103, 286–292.
- Sačkov, I., Hlásny, T., Bucha, T., Juriš, M., 2017. Integration of tree allometry rules to treetops detection and tree crowns delineation using airborne lidar data. *iForest-Biogeosci. Forestry* 10, 459.
- Shao, G., Reynolds, K.M., 2006. *Computer Applications in Sustainable Forest Management: Including Perspectives on Collaboration and Integration*. Springer Science & Business Media.
- Singh, K.K., Davis, A.J., Meentemeyer, R.K., 2015. Detecting understory plant invasion in urban forests using LiDAR. *Int. J. Appl. Earth Obs. Geoinf.* 38, 267–279.
- Solberg, S., Naesset, E., Bollandsas, O.M., 2006. Single tree segmentation using airborne laser scanner data in a structurally heterogeneous spruce forest. *Photogramm. Eng. Remote Sens.* 72, 1369–1378.
- Swatantran, A., Tang, H., Barrett, T., DeCola, P., Dubayah, R., 2016. Rapid, High-Resolution Forest Structure and Terrain Mapping over Large Areas using Single Photon Lidar. *Sci. Rep.* 6.
- Takahashi, T., Yamamoto, K., Miyachi, Y., Senda, Y., Tsuzuku, M., 2006. The penetration rate of laser pulses transmitted from a small-footprint airborne LiDAR: a case study in closed canopy, middle-aged pure sugi (*Cryptomeria japonica* D. Don) and hinoki cypress (*Chamaecyparis obtusa* Sieb. et Zucc.) stands in Japan. *J. For. Res.* 11, 117–123.
- Terrasolid Ltd., 2012. *TerraScan User's Guide*. In: *Terrasolid Oy*.
- Vastaranta, M., Holopainen, M., Yu, X., Hyyppä, J., Mäkinen, A., Rasinmäki, J., Melkas, T., Kaartinen, H., Hyyppä, H., 2011. Effects of individual tree detection error sources on forest management planning calculations. *Remote Sens.* 3, 1614–1626.
- Vauhkonen, J., Ene, L., Gupta, S., Heinzel, J., Holmgren, J., Pitkänen, J., Solberg, S., Wang, Y., Weinacker, H., Hauglin, K.M., 2011. Comparative testing of single-tree detection algorithms under different types of forest. *Forestry*. cpr051.
- Véga, C., Durrieu, S., 2011. Multi-level filtering segmentation to measure individual tree parameters based on Lidar data: Application to a mountainous forest with heterogeneous stands. *Int. J. Appl. Earth Obs. Geoinf.* 13, 646–656.
- Véga, C., Hamrouni, A., El Mokhtari, S., Morel, J., Bock, J., Renaud, J.-P., Bouvier, M., Durrieu, S., 2014. PTrees: A point-based approach to forest tree extraction from lidar data. *Int. J. Appl. Earth Obs. Geoinf.* 33, 98–108.
- Wallace, A., 2017. Leica's new airborne LiDAR offers 10x efficiency boost. In: *Spatial Source*.
- Wallace, L., Lucieer, A., Watson, C.S., 2014. Evaluating tree detection and segmentation routines on very high resolution UAV LiDAR data. *IEEE Trans. Geosci. Remote Sens.* 52, 7619–7628.
- Wang, Y., Weinacker, H., Koch, B., 2008. A lidar point cloud based procedure for vertical canopy structure analysis and 3D single tree modelling in forest. *Sensors* 8, 3938–3951.
- Weinacker, H., Koch, B., Heyder, U., Weinacker, R., 2004. Development of filtering, segmentation and modelling modules for lidar and multispectral data as a fundament of an automatic forest inventory system. *Int. Arch. Photogramm., Remote Sens. Spatial Inform. Sci.* 36 (Part 8), W2.
- Whitehurst, A.S., Swatantran, A., Blair, J.B., Hofton, M.A., Dubayah, R., 2013. Characterization of canopy layering in forested ecosystems using full waveform lidar. *Remote Sens.* 5, 2014–2036.
- Wing, B.M., Ritchie, M.W., Boston, K., Cohen, W.B., Gitelman, A., Olsen, M.J., 2012. Prediction of understory vegetation cover with airborne lidar in an interior ponderosa pine forest. *Remote Sens. Environ.* 124, 730–741.
- Wulder, M.A., White, J.C., Nelson, R.F., Næsset, E., Ørka, H.O., Coops, N.C., Hilker, T., Bater, C.W., Gobakken, T., 2012. Lidar sampling for large-area forest characterization: A review. *Remote Sens. Environ.* 121, 196–209.